

Effect of Bond Properties on the Behavior of FRP-Strengthened RC Girders Subjected to Monotonic and Cyclic Loads

by F. Lu and A. Ayoub

Synopsis: Externally bonded carbon fiber reinforced polymer (CFRP) is a feasible and economical alternative to traditional methods for strengthening and stiffening deficient reinforced and prestressed concrete bridge girders. The behavior of bond between FRP and concrete is the key factor controlling the behavior of these structures. Several experiments showed that debonding failure occurs frequently before FRP rupture and therefore the FRP strength can not be fully utilized. For design accuracy, the FRP strength must be reduced. This paper analyzes the effect of the bond properties on the response and failure modes of FRP-strengthened RC beams. A nonlinear RC beam element model with bond-slip between the concrete and the FRP laminates is used to analyze a test specimen subjected to monotonic and cyclic loads typical of seismic excitations, and to investigate the corresponding failure mode, and whether it is due to FRP rupture, debonding, or concrete crushing. The model is considered one of the earliest studies to numerically evaluate the behavior of FRP-strengthened girders under seismic loads. The model was also used to study the reduction factor of FRP tensile strength of simply supported strengthened RC girders due to debonding failure. This reduction factor seems to be directly affected by the bond strength between FRP and concrete interface. The study concludes with a numerical evaluation of the current ACI 440.2R guidelines for bond reduction factors.

Keywords: carbon fiber; debonding; degradation; finite element analysis; interface; laminates; seismic analysis

Feifei Lu is a Structural Engineer at Shaw Stone & Webster Inc., Charlotte, NC. She obtained her MS degree from the University of Missouri-Rolla. Her research interests include analysis and design of FRP composite structures.

ACI member **Ashraf Ayoub** is an Assistant Prof. in the Dept. of Civil, Arch., and Env. Engrg. at the University of Missouri-Rolla. He is a member of ACI committee 447, Finite Element Analysis of Reinforced Concrete Structures, and an associate member of ACI committee 440, Fiber Reinforced Polymer Reinforcement. His research interests include non-linear analysis of reinforced and prestressed concrete structures, and performance-based earthquake engineering.

INTRODUCTION

The use of Fiber-reinforced polymer (FRP) materials for flexural strengthening of reinforced concrete girders started in the late 1970s. Since then FRP strengthening was established as an efficient and economical technique for repair and rehabilitation of deteriorating RC structures. To understand the complex behavior and possible failure mechanisms of FRP composite structures, extensive experimental investigations were carried out by different researchers. Several failure modes were observed during these tests. These failure modes were classified in two types by Thomsen (2004)¹. Type one includes modes exhibiting composite action up to failure of the strengthened beam, which could be due to concrete crushing, FRP rupture, or lack of shear resistance. Type two, on the other hand, consists of failure due to loss of composite action. In this case either debonding between the FRP laminate and concrete surface is observed, or end peeling takes effect, where the concrete cover in the region near the supports peels off.

The expected failure mode of a strengthened RC girder depends on several parameters. These parameters include the FRP plate length, plate width, plate stiffness, and loading type among others. The experimental results, however, indicate that the most common failure mode is due to loss of composite action between the FRP and the concrete girder. In this case, debonding occurs before FRP rupture, and the FRP strength can not therefore be fully utilized. The ACI 440 guidelines² for flexural strengthening with FRP composites recognized this fact and introduced a bond reduction factor k_m for the FRP strength. This factor equals the effective FRP stress at failure divided by the original FRP strength. The development of the proposed values for the bond reduction factor k_m was based mainly on experimental investigations. Due to the large cost of experimental research, the proposed factor accounts only for a limited number of parameters, and doesn't take into account the value of the bond strength at the interface level. There exists a need to conduct an analytical investigation, where an evaluation of the parameters affecting the debonding failure is carefully examined. Before attempting to conduct this task, a brief review of recent work related to behavior and failure of RC girders strengthened with FRP plates is presented first.

Six RC strengthened beams with different wrapping schemes and layers of FRP were tested under monotonic loads³. The specimens showed three types of failure modes. The two-layer fully wrapped specimens failed after the fabric reinforcement fractured. The specimens reinforced with three and four layers of fabric failed suddenly after crushing of the concrete occurred. The partially wrapped specimens failed by delamination of the concrete below the longitudinal steel reinforcement. For fully wrapped specimens (one to four layers), ductility was reduced with increasing number of layers, probably due to failure of concrete in the compression regions. Furthermore, the partially wrapped specimens exhibited a very undesirable failure mode. As the applied load increased, a horizontal crack developed at the level of internal steel reinforcement, followed shortly by the delamination of concrete in the bottom portion of the beam.

Additional experimental tests where debonding failure was observed were also reported^{4,5}. End peeling was also observed in several studies^{4,6,7}. Other studies where failure was due to steel yielding followed by FRP rupture were conducted⁸. Shear failure was also observed in several studies⁹. These studies revealed that assessment of the expected failure mode of FRP-strengthened girders is rather complex.

The effect of bond on the overall behavior and failure of FRP composite structures prompted researchers to evaluate the bond stress-slip characteristics of the FRP-concrete interface. Several pull-out tests with different layers of CFRP laminates were conducted¹⁰. Failure occurred in the concrete-adhesive interface, with very little or no sign of damage in the concrete surface. The bonded length did not affect the ultimate load, thus confirming the existence of an effective length beyond which no additional stress is transferred. The number of plies used affected the failure load, but the average of the ultimate loads of specimens with two plies was only 1.5 times of that of specimens with one ply. Based on this work, a factor K , to evaluate the effective maximum FRP strain was introduced. This factor was a function of the FRP thickness and modulus only.

The influence of the concrete strength and the embedment length were analyzed in an experimental research¹¹. The bond strength (τ_{max}) proved to have a tendency to decrease with the increment of the embedment length. The influence of the concrete strength on maximum bond stress and reduction factor of FRP was marginal.

Several analytical models to describe the bond stress-slip behavior of FRP-concrete interface were proposed. A bond-slip model to quantify the different bonding mechanisms and describe the bond characteristics of FRP sheet-concrete interfaces was proposed^{12,13}. Near-end supported (NES) single-shear pull tests were conducted¹⁴. Another study used two bond stress-slip models, linear up to failure and bilinear models, along with a fracture mechanics-based approach to solve the stress transfer problem of pull-out specimens¹⁵. The study concluded that bilinear models give better correlation with experimental findings in describing both the interfacial bond stress distribution and the effective stress transfer length.

A critical review and assessment of different bond-slip models was presented by Lu et al. (2005)¹⁶. In this study, a set of three new bond-slip models were also proposed. A closed-form analytical solution for the bond slip analysis of beams strengthened with full or partial FRP wraps based on beam theory with a shear deformable adhesive layer was developed¹⁷. The results showed that the solution converges to the limiting cases of perfect bond and no bond using high and low interface shear modulus, respectively.

A non-linear finite element analysis of RC beam strengthened with externally bonded FRP plate was developed¹⁸. The local constitutive models of cracked concrete and shear transfer model were used to predict load-deformation relation, ultimate load, and even the failure mode of the beam. The FEM analysis could also capture the cracking process for both shear-flexural peeling and end peeling modes, similar to the experiment results.

A series of shallow RC beams strengthened with steel and FRP plates were analyzed¹⁹. The study relies on a simple and accurate displacement-based fiber frame element with bond slip between the RC beam and the strengthening plate. The results of the analysis showed that failure of the strengthened RC beams was always initiated by plate debonding. Debonding occurred somewhere between the point of load application and the plate end.

RESEARCH SIGNIFICANCE

The objective of the study is to evaluate the effect of the bond properties on the behavior and failure mode of FRP-strengthened concrete girders subjected to monotonic and cyclic loading conditions. Evaluation of ACI-440 specifications for bond reduction factors is also conducted. In order to simulate the nonlinear response of FRP-strengthened concrete members under both monotonic and cyclic loads, a nonlinear finite element model capable of simulating all possible failure modes is presented in this paper. The model is based on fiber discretization, and is described in the next section. The model is considered one of the earliest studies aimed at numerically evaluating the behavior of FRP-strengthened girders under seismic loads. The model was added to the library of elements of the finite element program FEAP²⁰.

FINITE ELEMENT FORMULATION OF FRP-STRENGTHENED RC BEAMS

The finite element formulation of the FRP-strengthened beam starts by considering the strong form equations of the problem. The model accounts for the bond-slip behavior at the interface between the concrete and FRP sheets, but neglect shear deformations. The equilibrium equations of the element are presented first.

Equilibrium

Consider an element of length dx of an RC beam section reinforced with one sheet, as shown in [Figure \(1\)](#). The equations of equilibrium for the beam are:

Concrete beam

$$N_{c,x} = bq$$

$$V_{,x} = -w_y \quad (1-a)$$

$$M_{,x} = -V + hN_{c,x}$$

FRP sheet

$$N_{FRP,x} = -bq \quad (1-b) \quad (1)$$

where N_c , and N_{FRP} are the axial forces in the concrete and FRP sheet respectively, q_b is the bond stress, b is the section width, w_y is the applied external load, V is the shear force, M is the bending moment, h is the distance between the resultant concrete compressive stresses and the FRP sheet, and a comma denotes derivation.

The total external moment, M_t , will be resisted by the moment in the concrete beam, M , plus the couple arising from the axial forces in the concrete and FRP sheet, which are equal:

$$M_t = M - hN_c \quad (2)$$

Substituting in (1-a), we get:

$$M_{t,xx} = -w_y \quad (3)$$

120 Lu and Ayoub

Equations (1-3) represent the equilibrium equations of the axial and flexural forces, respectively. Writing the equilibrium equations in matrix form:

$$\mathbf{L}^T \mathbf{D}(x) - \mathbf{L}_b^T b \mathbf{q}(x) = \mathbf{w} \quad (4)$$

where

$$\mathbf{D}(x) = [N_c(x) \quad N_{FRP}(x) \quad M(x)]^T \quad (5)$$

$$\mathbf{L} = \begin{bmatrix} d/dx & & \\ & d/dx & \\ & & d^2/dx^2 \end{bmatrix} \quad (6)$$

$$\mathbf{L}_b = [1 \quad -1 \quad hd/dx] \quad (7)$$

$$\mathbf{w} = [0 \quad 0 \quad w_y]^T \quad (8)$$

\mathbf{L} is a 3x3 differential operator, \mathbf{L}_b is a 1x3 differential operator, b is the beam width, and \mathbf{w} is a 1x3 load vector.

Compatibility:

The compatibility equations relate the strain in both the FRP sheet and concrete to the derivative of their corresponding axial displacement, and the section curvature to the second derivative of the transverse displacement. They are grouped in the following matrix form:

$$\mathbf{L}\mathbf{u}(x) - \mathbf{d}(x) = 0 \quad (9)$$

where

$$\mathbf{u}(x) = [u_c(x) \quad u_{FRP}(x) \quad v(x)]^T \quad (10)$$

and

$$\mathbf{d}(x) = [\varepsilon_c(x) \quad \varepsilon_{FRP}(x) \quad \chi(x)]^T \quad (11)$$

u_c is the concrete axial displacement, u_{FRP} is the FRP axial displacement, v is the transverse displacement, ε_c is the concrete axial strain, ε_{FRP} is the FRP axial strain, and χ is the curvature. \mathbf{L} is the differential operator defined in (4).

The slip between the FRP sheet and the concrete bottom fiber $S_b(x)$ is calculated as follows:

$$S_b(x) = \mathbf{L}_b \mathbf{u}(x) \quad (12)$$

Where \mathbf{L}_b is as defined in (4).

Constitutive laws:

The present model uses fiber discretization to describe section behavior, and an interface element to model bond between FRP and concrete. The section constitutive law is:

$$\mathbf{D}(x) = f_{sec}[\mathbf{d}(x)] \quad (13)$$

where $\mathbf{D}(x)$ and $\mathbf{d}(x)$ are as defined before, and f_{sec} is a nonlinear function that describes the section force deformation response. The section force deformation relation is determined through fiber integration. The fibers are either concrete, steel, or FRP.

The bond constitutive law for the interface between FRP and concrete is:

$$q_b(x) = f_{bond}[S_b(x)] \quad (14)$$

where $q_b(x)$ and $S_b(x)$ are as defined before, and f_{bond} is a nonlinear function that describes the bond stress slip relation.

Material constitutive laws for the main components of the FRP-strengthened reinforced concrete beam, namely steel, concrete, FRP and bond have to be accurately determined. The concrete uniaxial constitutive law used is based on the model by Kent and Park²¹. The model accounts for successive stiffness degradation for both the unloading

and reloading branches, as shown in Figure (2). The steel uniaxial stress-strain law used is based on the model by Menegotto and Pinto²² as modified by Filippou et al.²³ to include isotropic hardening. The model, shown in Figure (3), accounts for Bauschinger effects under reversed loading and in general has proven to agree well with experimental results of reinforcing bars under cyclic loading conditions. The FRP laminate is modeled as elasto-brittle material. The stress is linear up to the tensile strength and drops sharply to zero, representing the fracture of the FRP laminate as shown in Figure (4).

Bond stress-slip relations are usually based on data from experiments such as pull-out tests. For the bond between the concrete and the FRP strengthening plate, a 3 stage multi-linear model was proposed^{13,16}, as show in Figure (5). This model proved to agree well with experimental results, and was used successfully by various researchers. The behavior of the interfacial bond under cyclic loads typically follows a stiffness degrading pinching model²⁴. A pinching model that accounts for stiffness and strength degradation under cyclic load reversals is proposed in this study, and is shown in Figure (6). The parameters α and k used in the model are typically assumed to equal 0.5. The model was used in several earlier studies^{25,26}, and agree well with data obtained from cyclic pull-out tests of FRP sheets²⁷, as shown in Figures (7) and (8).

Finite Element Formulation

In a nonlinear finite element formulation, the structure is subdivided into discrete elements. Consistent linearization of the governing differential equations for a single element is used to derive the element stiffness matrix and resisting load vector. The structure stiffness matrix and resisting load vector is then assembled from the element contributions following well established principles of structural analysis. The resulting system of equations is solved by an iterative solution strategy, commonly of Newton-Raphson type. In this solution strategy, the linearized system of equations about the current state of the structure is solved for the unknown increments of the primary variables. The iteration continues until convergence is satisfied within a specified tolerance. The solution then advances to the next load step. The formulation for a single Newton-Raphson iteration denoted by i is based on the following steps:

- (1) Assuming a predefined displacement field $\mathbf{u}(x)$ along the finite element

$$\mathbf{u}(x) = \mathbf{a}(x) \mathbf{v} \quad (15)$$

where $\mathbf{u}(x)$ is the vector of displacements at point x defined in (9), $\mathbf{a}(x)$ is a 3 by n_d matrix of displacement interpolation functions, n_d is the number of degrees of freedom of the finite element, and \mathbf{v} is the vector of displacement degrees of freedom of the finite element.

- (2) Deriving the weighted integral form of the equilibrium equations

$$\int_0^L \delta \mathbf{u}^T(x) [\mathbf{L}^T \mathbf{D}^i(x) - \mathbf{L}_b^T b \mathbf{q}^i(x) - \mathbf{w}] dx = 0 \quad (16)$$

where $\delta \mathbf{u}(x)$ is a weighting function. For the sake of simplicity the effect of element loads \mathbf{w} is not pursued further in this study. Integrating by parts twice the first term in (16), and substituting the incremental force-deformation relation of the section and bond interface respectively results in

$$\int_0^L \mathbf{L}^T \delta \mathbf{u}^T(x) [\mathbf{k}_s^{i-1} \Delta \mathbf{d}^i + \mathbf{D}^{i-1}] dx + \int_0^L \mathbf{L}_b^T \delta \mathbf{u}^T(x) [b \mathbf{k}_b^{i-1} \Delta \mathbf{S}_b^i + b \mathbf{q}^{i-1}] dx = BT \quad (17)$$

where \mathbf{k}_s and \mathbf{k}_b are the section and bond stiffness terms respectively and are evaluated from the functions f_{sec} and f_{bond} respectively, BT is a boundary term, and \mathbf{D} and \mathbf{q} are the section and bond resisting loads respectively.

- (3) Substituting the predefined displacement shape functions into the weak form (17), and using a Galerkin approach for the weighting functions yields

$$(\mathbf{K}_s^{i-1} + \mathbf{K}_b^{i-1}) \Delta \mathbf{u}^i = \mathbf{P} - \mathbf{Q}_s^{i-1} - \mathbf{Q}_b^{i-1} \quad (18)$$

Where

$$\mathbf{K}_s^{i-1} = \int_0^L \mathbf{B}^T(x) \mathbf{k}_s^{i-1}(x) \mathbf{B}(x) dx \quad (19)$$

$$\mathbf{K}_b^{i-1} = \int_0^L \mathbf{B}_b^T(x) \rho k_b^{i-1}(x) \mathbf{B}_b(x) dx \quad (20)$$

$$\mathbf{Q}_s^{i-1} = \int_0^L \mathbf{B}^T \mathbf{D}^{i-1}(x) dx \quad (21)$$

$$\mathbf{Q}_b^{i-1} = \int_0^L \mathbf{B}_b^T(x) \rho \mathbf{q}^{i-1}(x) dx \quad (22)$$

$$\mathbf{B}(x) = \mathbf{L} \mathbf{a}(x) \quad (23)$$

$$\mathbf{B}_b(x) = \mathbf{L}_b \mathbf{a}(x) \quad (24)$$

\mathbf{K}_s^{i-1} is the section element stiffness matrix, \mathbf{K}_b^{i-1} is the bond interface element stiffness matrix, \mathbf{Q}_s^{i-1} is the section element resisting load vector, \mathbf{Q}_b^{i-1} is the bond interface element resisting load vector; $\mathbf{B}(x)$, $\mathbf{B}_b(x)$ and \mathbf{P} is the vector of applied external loads.

VALIDATION OF ANALYTICAL MODEL

To validate the finite element model, a correlation study with the specimen tested at the University of Ljubljana, Slovenia, by Zarnic and his coworkers⁵ is conducted.

The material properties and geometry of the specimen are shown in Tables (1) and (2) and Figure (9). The CFRP plates were 50 mm wide and 1.2 mm thick. The symmetry is taken advantage of by simulating only half of the beam. A total of 12 finite elements are used along the beam in order to obtain accurate and detailed results.

According to the mechanical properties of the epoxy resin used in the experimental tests⁵, a bond elastic stiffness of 2,384 MPa/mm was assumed for the numerical investigation. The bond strength was assumed to equal 5.0 MPa.

Figure (10) shows the experimental load-deformation⁵ and the numerical results provided by Thomsen et al.¹, while Figure (11) shows the analytical results using the proposed model. By comparing Figures (10) and (11), it is rather obvious that the numerical load-deformation results of the CFRP strengthened RC beam matches well with the experimental results.

Figure (12) shows the bond force distribution along the FRP-concrete interface provided by Thomsen et al.¹. The bond force per unit length equals the bond stress times the width of the section. Figure (13) shows the analytical bond stress distribution using the proposed finite element model. In both Figures (12) and (13), it was observed that the maximum value of bond stress occurred in the region near the point of load application.

The analysis of the specimen was repeated under cyclic loading conditions expected during seismic excitations. The resulting load-deformation behavior is shown in Figure (14). The response clearly revealed a degradation in strength under cyclic load reversals.

CURRENT SPECIFICATIONS FOR BOND REDUCTION FACTOR

Before the discussion of the effect of the bond properties on the behavior of FRP-strengthened girders, the k_m bond reduction factor will be introduced according to the guidelines of committee ACI-440² (ACI 440.2R-02). k_m is a reduction factor of FRP ultimate strength due to debonding failure. In order to prevent debonding of the FRP laminate, a limitation is placed on the strain level developed in the laminate. Equation (25) and (26) give the expression for the bond-dependent coefficient k_m .

$$k_m = \begin{cases} \frac{1}{60\varepsilon_{fu}} \left(1 - \frac{nE_f t_f}{2,000,000} \right) \leq 0.90 \text{ for } nE_f t_f \leq 1,000,000 \\ \frac{1}{60\varepsilon_{fu}} \left(\frac{500,000}{nE_f t_f} \right) \leq 0.90 \text{ for } nE_f t_f > 1,000,000 \end{cases} \text{-----US} \quad (25)$$

$$k_m = \begin{cases} \frac{1}{60\epsilon_{fu}} \left(1 - \frac{nE_f t_f}{360,000} \right) \leq 0.90 & \text{for } nE_f t_f \leq 180,000 \\ \frac{1}{60\epsilon_{fu}} \left(\frac{90,000}{nE_f t_f} \right) \leq 0.90 & \text{for } nE_f t_f > 180,000 \end{cases} \text{-----SI} \quad (26)$$

The term k_m , expressed in Equation (25) and Equation (26), is a factor no greater than 0.90 that may be multiplied by the rupture strain of the FRP laminate to reach a strain limitation to prevent debonding. The k_m factor equals f_{fe}/f_{fu} , where f_{fe} is the maximum FRP stress at debonding and f_{fu} is the FRP design strength. The number of plies n used in this equation is the number of plies of FRP flexural reinforcement at the location along the length of the member where the moment strength is being computed. This term recognizes that laminates with greater stiffnesses are more prone to delamination. Thus, as the stiffness of the laminate increases, the strain limitation becomes more severe. For laminates with a unit stiffness $nE_f t_f$ greater than 1,000,000 lb/in (180,000 N/mm), k_m places an upper bound on the total force that can be developed in the laminate, regardless of the number of plies. The width of the FRP laminate is not included in the calculation of the unit stiffness, $nE_f t_f$, because an increase in the width of the FRP results in a proportional increase in the bond area. The k_m term is only based on a generally recognized trend and on the experience of engineers practicing the design of bonded FRP systems.

ACI 440 is currently developing new specifications for bond reduction factor. Accordingly, the FRP strain level at which debonding may occur, ϵ_{fd} is evaluated as follow:

$$\epsilon_{fd} = 0.083 \sqrt{\frac{f'_c}{nE_f t_f}} \leq 0.9\epsilon_{fu} \text{-----US} \quad (27)$$

$$\epsilon_{fd} = 0.41 \sqrt{\frac{f'_c}{nE_f t_f}} \leq 0.9\epsilon_{fu} \text{-----SI} \quad (28)$$

The effective FRP stress, f_{fe} , in case failure is governed by debonding is:

$$f_{fe} = E_f \epsilon_{fd} \quad (29)$$

Both, the original and new expressions, do not take into account the properties of the bond interface between the FRP and concrete.

BOND BETWEEN FRP AND CONCRETE SURFACE

There are several factors that can affect the bond stress between the FRP and concrete surface, such as the adhesive properties and the surface preparation. The ultimate bond stress is the key parameter that determines when the debonding failure occurs, and directly affects the value of f_{fe}/f_{fu} . From experimental pull-out tests, the ultimate bond stress typically varies from 2 MPa to 6 MPa.

In order to assess the effect of the ultimate bond stress on the behavior and failure mode of FRP-strengthened girders, a series of numerical studies on a representative specimen is undertaken using the proposed finite element model. The selected specimen has the same geometry as the one tested in [5] and described earlier. The specimen is analyzed under different bond strength values. For each case, the value of the bond reduction factor k_m is evaluated as the ratio of the recorded FRP stress to the FRP strength.

Figure (15) shows that the load-deformation response of the beams with different bond strength values follows the same equilibrium path, varying only at the point of failure. The bond stress-slip behavior in this case is assumed to be elasto-brittle up to the bond stress which is referred to as bond model I, following the assumption of Thomsen et al. in [1]. The elastic bond stiffness was assumed to equal 2384 MPa/mm¹⁰. Figure (16) shows the value of f_{fe}/f_{fu} for different values of ultimate bond stress, varying from 2 MPa to 5 MPa. The value of f_{fe}/f_{fu} is almost linearly increasing when the bond stress increases. The analysis for the case of an ultimate bond stress greater than 5 MPa is not show in this figure, because in this case, concrete failure occurs before debonding failure.

The previous analysis is repeated taking into account the bond ductility. The trilinear bond stress-slip model was therefore used, which is referred to as bond model II. The hardening slope was assumed to equal 1%, and the slip at the start and end of the softening branch were assumed to equal 0.12 mm and 0.3 mm respectively ¹⁰. Figure (17)

shows the response of the strengthened beam with increasing values of bond strength. The plot revealed that the bond ductility did not have an effect on the global response of the beam. It did have an effect though on the observed failure mode and the effective FRP stress, since it allowed for excessive slip values to occur along the beam length. **Figure (18)** shows the value of f_{fe}/f_{fu} for different ultimate bond stresses ranging from 2 MPa to 3 MPa. The value of f_{fe}/f_{fu} was larger than that of the brittle bond, although it also shows a linearly increasing trend. However, when the bond strength is larger than 3 MPa, it was observed that failure was governed by concrete crushing rather than debonding.

In order to evaluate the effect of degradation on the f_{fe}/f_{fu} ratio, the analysis using bond model II is repeated under cyclic loads expected during seismic excitations. **Figure (19)**, which shows the response with increasing values of bond strength, revealed that the strengthened beams also followed the same equilibrium path, varying only at the point of failure. **Figure (20)** shows the value of f_{fe}/f_{fu} in this case for different ultimate bond stresses ranging from 2 MPa to 3 MPa. The figure revealed that degradation under cyclic loads had a much greater effect on specimens with low bond strength than on those with higher bond strength values.

EVALUATION OF ACI-440 GUIDELINES

Figure (21) presents a comparison between the computed values of f_{fe}/f_{fu} for the given specimen as a function of the interface bond strength, and the k_m expression given by ACI-440.2R-02. While the ACI-440 equation accounts for $nE_f t_f$, it does not account for the bond strength between FRP and concrete. Therefore, the bond reduction factor evaluated using ACI-440 guidelines in this case is constant and equals $k_m=0.41$. The value of f_{fe}/f_{fu} evaluated numerically however, varies as a function of the bond strength. For the ductile bond model, the computed k_m factor is higher than the one evaluated using the original ACI-440 expression by 0.08 if the bond strength equals 2 MPa, and by 0.2 if the bond strength equals 3 MPa. Failure in the case of a bond strength greater than 3 MPa is typically due to concrete crushing. If cyclic degradation is accounted for, the computed values are higher than the ACI-440 values by 0.01 and 0.18 if the bond strength is 2 MPa and 3 MPa respectively. These results show that the original ACI-440 guidelines seem to be on the conservative end if compared to the values using a ductile bond model. For the brittle bond model, the computed k_m values seem to be lower than those evaluated using ACI-440 guidelines. In this case, the ACI-440 guidelines appeared to be on the un-conservative end. The new expression proposed by ACI 440 appears to be even more conservative, as it predicts a k_m value of 0.27.

SUMMARY AND CONCLUSIONS

The paper analyzes the effect of the bond properties on the response and failure modes of FRP-strengthened RC beams subjected to monotonic and cyclic loading conditions. A nonlinear RC beam element model with bond-slip between the concrete and the FRP laminates was developed and used to analyze a beam specimen in order to evaluate the current bond design specifications for RC bridge beams strengthened with FRP laminates.

The following conclusions can be drawn from the study:

- The original ACI-440 expression for bond reduction factors seems to be on the conservative end if compared to the results of a trilinear bond stress-slip model, while it appears to be on the un-conservative end if compared to the results using an elasto-brittle bond model. The new expression proposed by ACI 440 appears to be even more conservative. If bond ductility is considered, it appears that a more efficient use of FRP could be allowed than what currently is being proposed.
- The bond strength of the interface between the FRP sheets and concrete surface has a great effect on the value of the bond reduction factor.
- Cyclic degradation expected during seismic excitations appears to have a great effect on the value of the bond reduction factor, particularly for specimens with low bond strength values. This effect needs to be accounted for in design guidelines.
- As evidenced by several numerical studies, larger ultimate bond stress allows a more efficient use of FRP. Once the ultimate bond stress exceeds a specific value, the failure mode tends to occur due to concrete crushing or FRP rupture.
- The current study, however, was based on analysis of a specific specimen with rectangular section. Further numerical studies on specimens with different geometries and cross sections, and additional correlations with experimental data are needed before confirming the accuracy of the given results. Furthermore, accurate evaluation using advanced experimental techniques of the value of the bond strength at the interface between the FRP and concrete is necessary in order to better calibrate the analytical model.

Acknowledgements

The authors greatly acknowledge the financial support provided by the NSF Industry-University Cooperative Research Center for Repair of Buildings and Bridges with Composites (RB²C) located at the University of Missouri-Rolla.

REFERENCES

1. Thomsen, H., Spacone, E., Limkatanyu, S. and Camata, G. (2004) "Failure Mode Analyses of Reinforced Concrete Beams Strengthened in Flexure with Externally Bonded Fiber-Reinforced Polymers." *Journal of Composites for Construction*, 8: 123–131.
2. ACI Committee 440 (2002) "Guide for the Design and Construction of Externally Bonded FRP Systems for Strengthening Concrete Structures" (440.2R-02), American Concrete Institute, Farmington Hills, Michigan.
3. Shahawy, M., and Beitelman, T. (1999). "Static and fatigue Performance of RC Beams Strengthened with CFRP Laminates", *Journal of Structural Engg*, 125(6): 613-621.
4. Tumialan, G., Serra, P., Nanni, A., and Belarbi, A. (1999). "Concrete cover delamination in RC beams strengthened with FRP sheets." *Proc., 4th Int. Symp. on FRP for Reinforcement of Concrete Structures*, American Concrete Institute, Detroit, 725–735.
5. Zarnic, R., Gostic, S., Bosiljkov, V., and Bokan, V. (1999). "Improvement of bending load-bearing capacity by externally bonded plates." *Proc., Creating with Concrete*, R. K. Dhir and N. A. Henderson, eds., Thomas Telford, London, 433–442.
6. Fanning, P., and Kelly, O. (2001). "Ultimate response of RC beams strengthened with CFRP plates." *Journal of Composites for Construction*, 5(2), 122–127.
7. Sebastian, W. (2001). "Significance of midspan debonding failure in FRP-plated concrete beams." *Journal of Structural Engineering*, 127(7), 792–798.
8. Bonacci, J. F., and Maalej, M. (2001). "Behavioral trends of RC beams strengthened with externally bonded FRP." *Journal of Composites for Construction*, 5(2), 102–113.
9. Seim, W., Hormann, M., Karbhari, V., and Seible, F. (2001). "External FRP poststrengthening of scaled concrete slabs." *Journal of Composites for Construction*, 5(2), 67–75.
10. Lorenzis, L.D., Miller B. and Nanni, A. (2001) "Bond of FRP to Concrete." *ACI Materials Journal*, 98: 256-264.
11. Sena-Cruz, J.M. and Barros, J.A.O. (2002) "Bond Behavior of Carbon Laminate Strips into Concrete by Pullout-Bending Tests." *Proceedings of the International Symposium "Bond in Concrete - from the Research to Standards"*, 614-621.
12. Dai, J. (2002) "Interfacial Models for Fiber Reinforced Polymer (FRP) Sheets Externally Bonded to Concrete."
13. Ueda, T. and Dai, J. (2005) "Interface Bond between FRP Sheets and Concrete Substrates: Properties, Numerical Modeling and Roles in Member Behaviour." *Prog. Struct. Engng Mater*, 7: 27-43.
14. Yao, J., Teng, J.G. and Chen, J.F. (2005) "Experimental Study on FRP-to-Concrete Bonded Joints." *Composites: Part B*, 36:99-113.
15. Wu, Z., Yuan, H., Yoshizawa, H. and Kanakubo, T. (2001) "Experimental / Analytical Study on Interfacial Fracture Energy and Fracture Propagation Along FRP-Concrete Interface." *Fracture Mechanics for Concrete Materials*, ACI International SP-201, September 2001, pp. 133-152.
16. Lu, X.Z., Teng, J.G., Ye, L.P. and Jiang, J.J. (2005) "Bond-Slip Models for FRP Sheet/Plate-to-Concrete Interfaces." *Engineering Structures*, 27: 938-950.
17. Rasheed, H.A. and Pervaiz, S. (2002) "Bond Slip Analysis of Fiber-Reinforced Polymer-Strengthened Beams." *Journal of Engineering Mechanics*, 128: 78-86.
18. Supaviriyakit, T., Pornpongsaroj, P., and Pimanmas, A. (2004) "Finite Element Analysis of FRP-Strengthened RC Beams." *Songklanakarinn Journal of Science and Technology*, 26: 497-507.
19. Aprile A., Spacone, E. and Limkatanyu, S. (2001) "Roles of Bond RC Beams Strengthened with Steel and FRP Plates." *Journal of Structural Engg*, 127: 1445-1452.
20. Zienkiewicz, O. C., and Taylor, R. L. (1989) "The Finite Element Method Volume 1. Basic Formulation and Linear Problems", Fourth Edition. McGraw Hill, London.
21. Kent, D.C., and Park, R. (1971). "Flexural Members with Confined Concrete." *J. Struct. Engrg., ASCE*, Vol. 97, No ST7, pp. 1969-1990.
22. Menegotto, M., and Pinto, P.E. (1973). "Method of analysis for cyclically loaded reinforced concrete plane frames including changes in geometry and nonelastic behavior of elements under combined normal force and bending." *Proc. IABSE Symposium on Resistance and Ultimate Deformability of Structures Acted on by Well-Defined Repeated Loads*, Final Report, Lisbon, Portugal.

126 Lu and Ayoub

23. Filippou, F.C., Popov, E.P., and Bertero, V.V. (1983). "Effects of bond deterioration on hysteretic behavior of reinforced concrete joints". Report No. UCB/EERC-83/19, Earthquake Engineering Research Center, University of California, Berkeley.
24. Elgehausen, R., Popov, E.P., and Bertero, V.V. (1983). "Local bond stress-slip relationships of deformed bars under generalized excitations". Report No. UCB/EERC 83/23, Earthquake Engineering Research Center, University of California, Berkeley, p. 178
25. Ayoub, A.S., Chenouda, M., and Mijo, C. (2004). "Displacement estimates and collapse prediction of degrading structural systems", Proceedings of the 13th world conference on earthquake engineering, paper # 2618.
26. Ayoub, A.S. (2007). "Nonlinear Analysis of wood building structures", Journal of Engineering Structures 29(2): 213-223.
27. Ko, H., and Sato, Y. (2007). "Bond stress-slip relationship between FRP sheet and concrete under cyclic load", *Journal of Composites for Construction*, 11(4): 419-426.

Table 1 - CFRP Properties

| Property | Value | Units |
|-----------------------|-------|-------|
| Tensile strength | 1800 | MPa |
| Modulus of elasticity | 140 | GPa |
| Thickness | 1.2 | mm |

Table 2 - Section and Material Properties

| Property | Value | Units |
|----------|-------|-----------------|
| A_s | 339 | mm ² |
| A_s' | 226 | mm ² |
| f_y | 460 | MPa |
| E_s | 210 | GPa |
| f'_c | 25 | MPa |
| E_c | 25 | GPa |

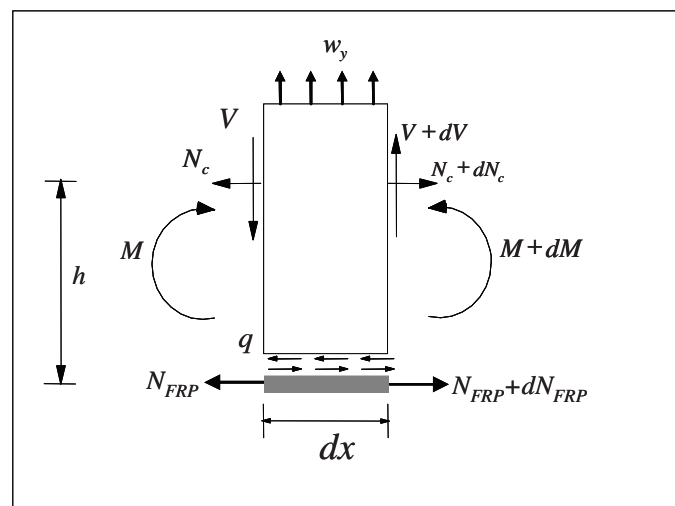


Figure 1 - Reinforced Concrete Beam Segment Strengthened with FRP Sheet

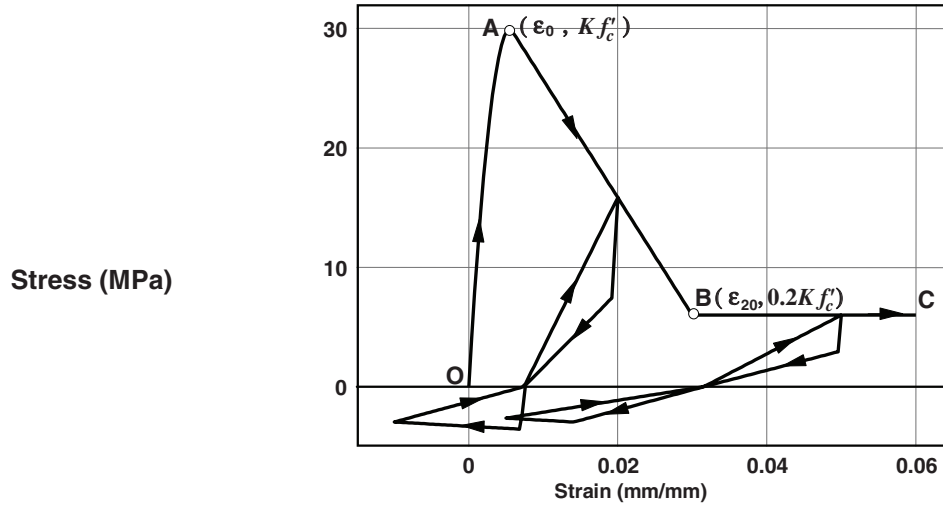


Figure 2 - Kent and Park Concrete Uniaxial Material Model in Compression

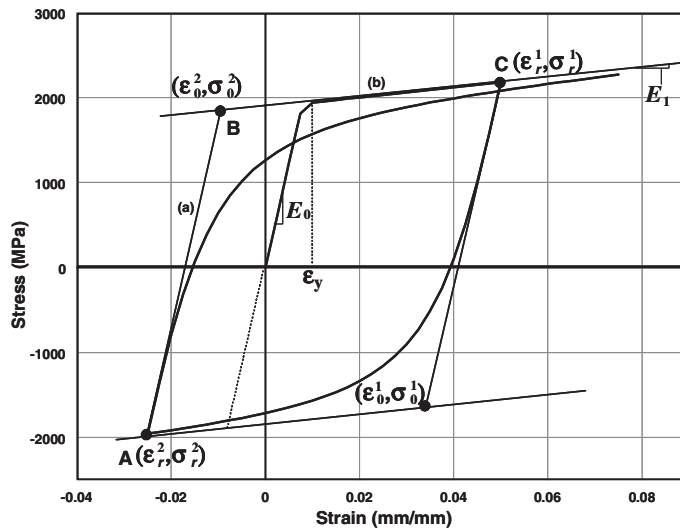


Figure 3 - Menegotto-Pinto Steel Model

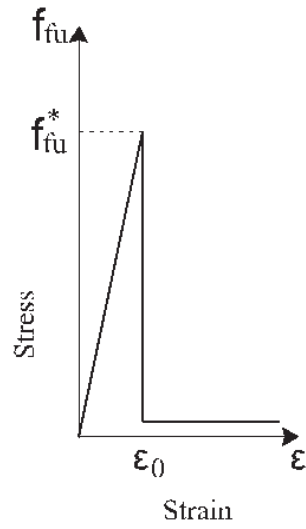


Figure 4 - FRP Model

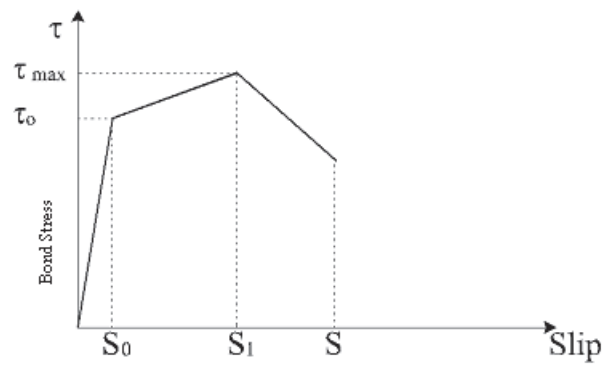


Figure 5 - Bond-Slip Monotonic Model

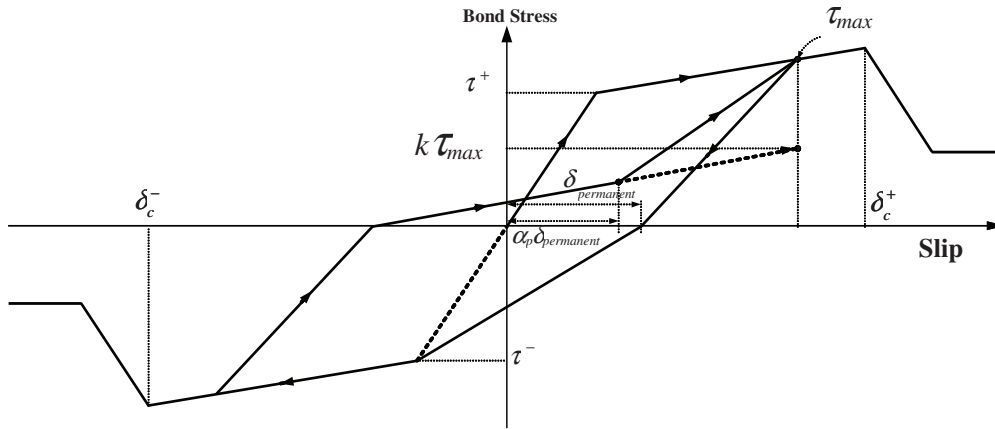


Figure 6 - Bond-Slip Cyclic Model

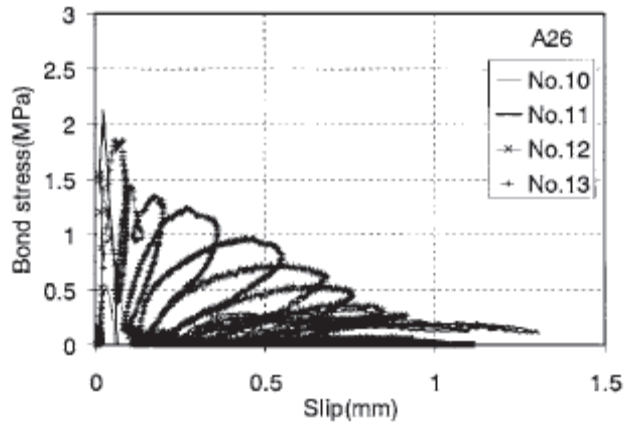


Figure 7 – Experimental Cyclic Bond Stress-Slip Relationship (from [27])

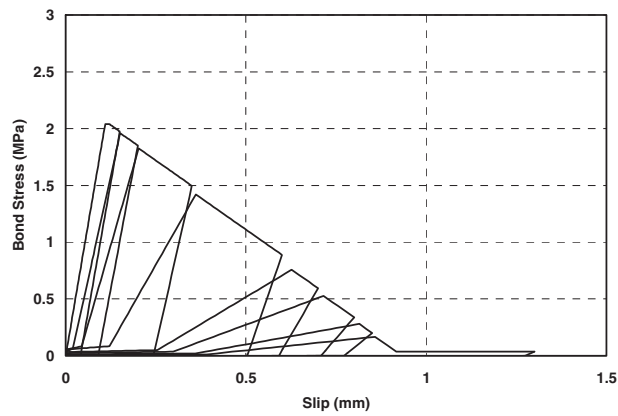
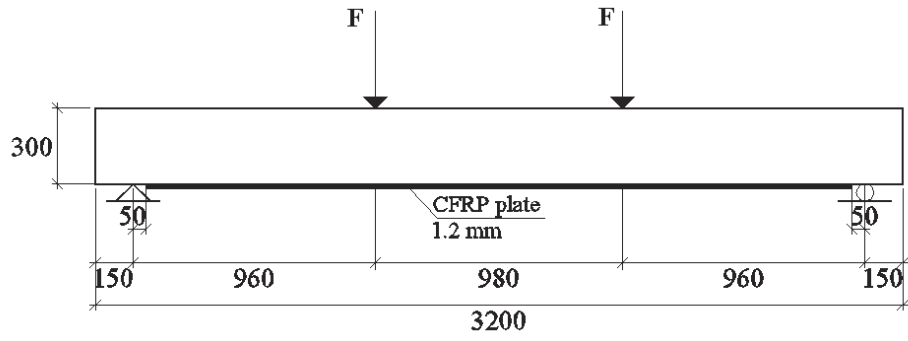
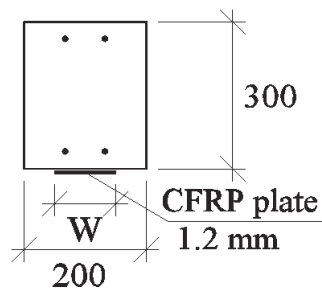


Figure 8 – Analytical Cyclic Bond Stress-Slip Relationship



STRAND PROFILE STRUCTURE
(Units:mm)



CROSS SECTION
(Units:mm)

Figure 9 - Section and Geometry Information of Zarnic RC Beam

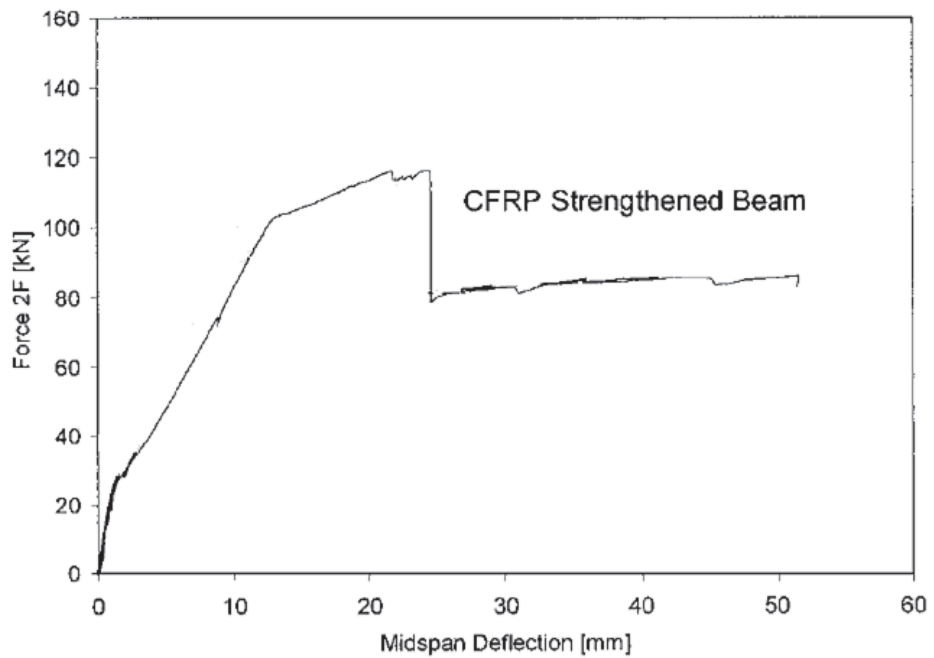


Figure 10 - Experimental Response of RC Beam (from [1])

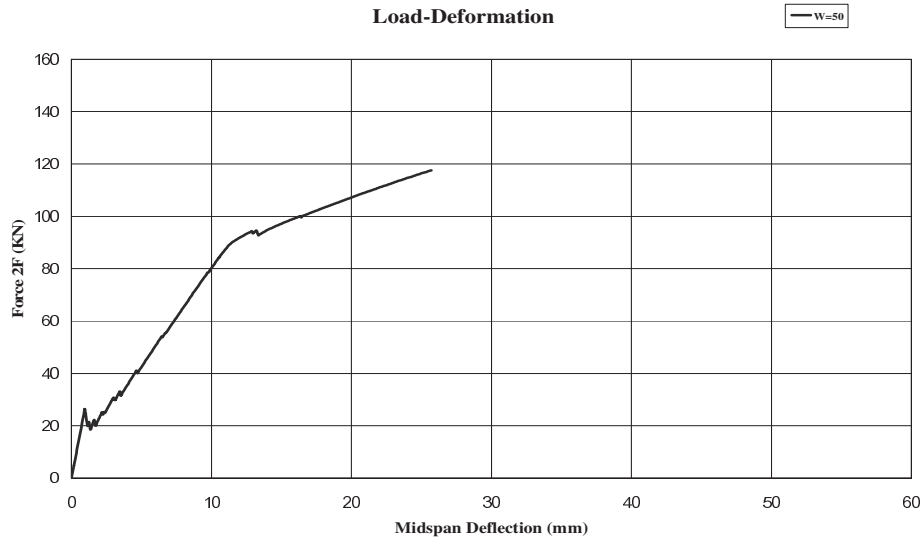


Figure 11 - Numerical Response of RC Beam

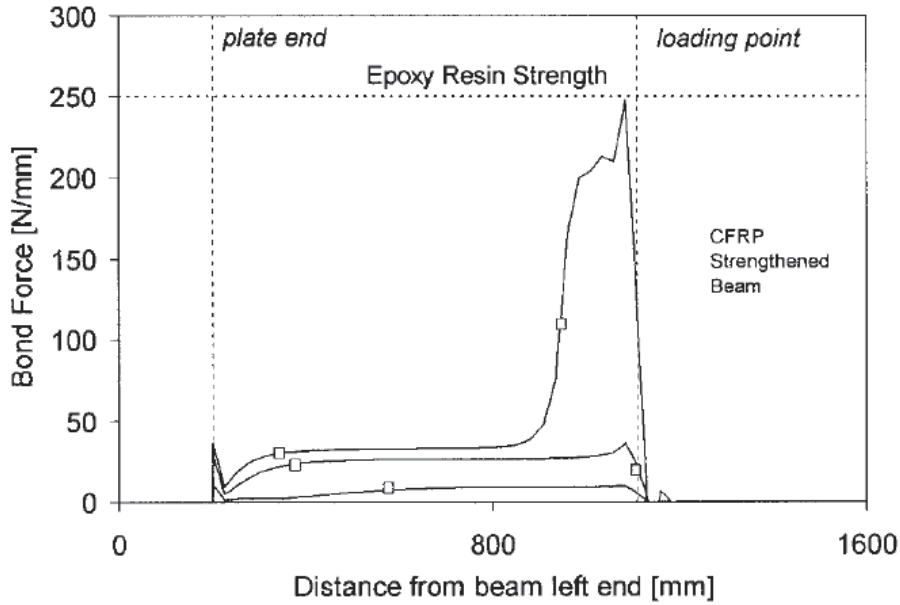


Figure 12 - Bond Force Distribution by Thomsen et al. (2004) (from [1])

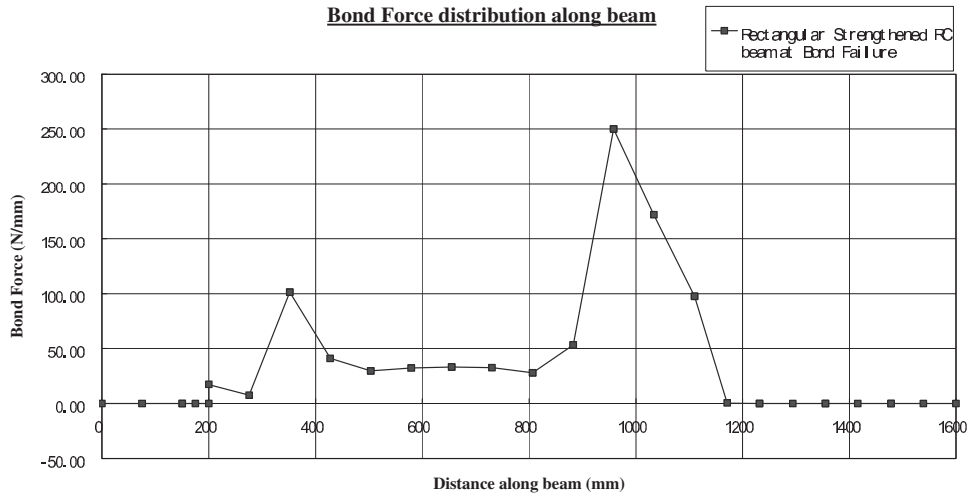


Figure 13 - Bond Force Distribution using Proposed Model

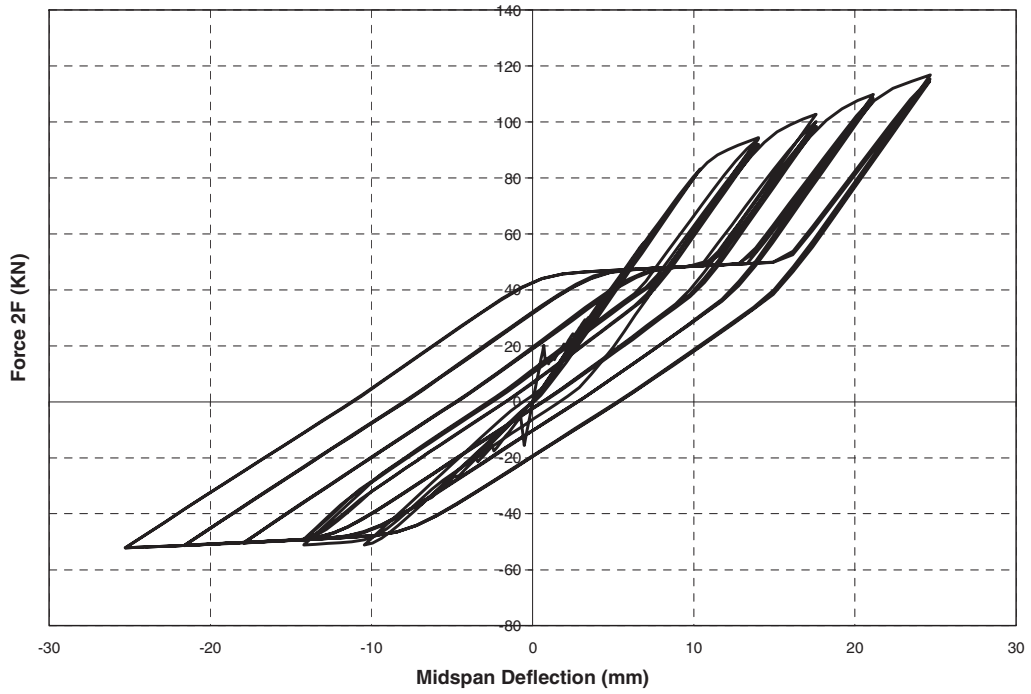


Figure 14 - Cyclic Response of Zarnic RC Beam

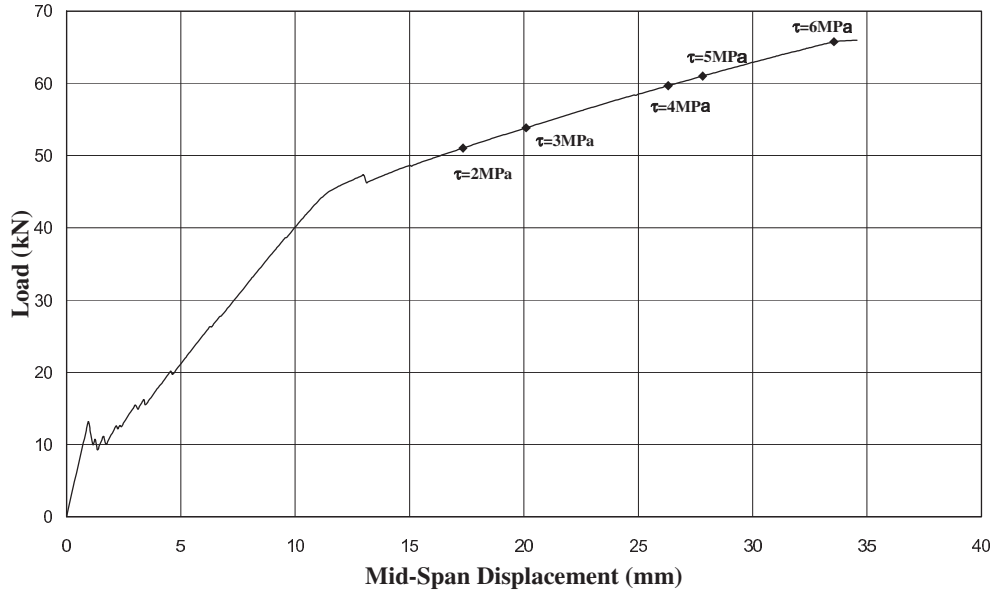


Figure 15 - Load- Deformation Response with Different Bond Strength Values

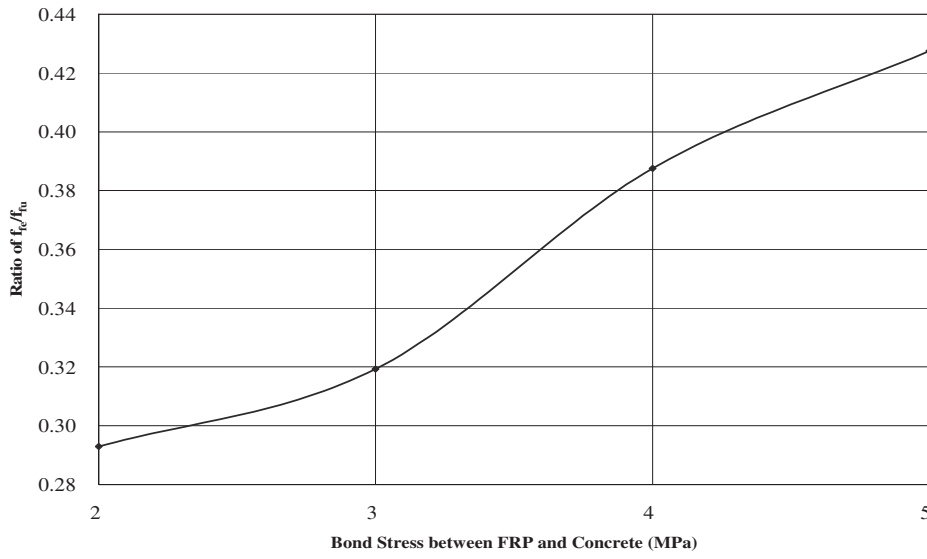


Figure 16 - Relationship of Bond Stress and Value of f_{fc}/f_{fu} (Brittle Bond)

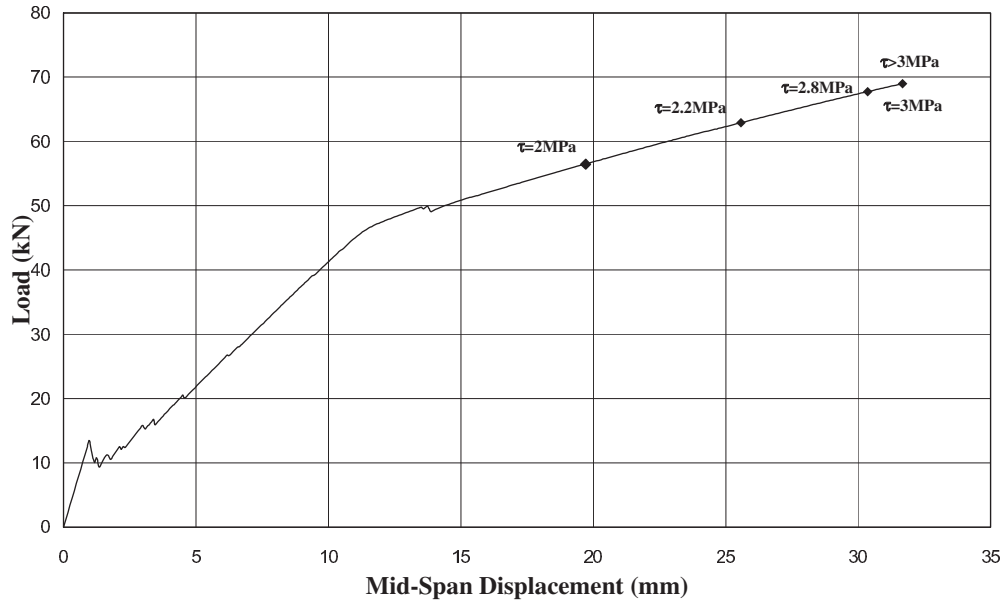


Figure 17 - Load- Deformation Response with Different Bond Strength Values

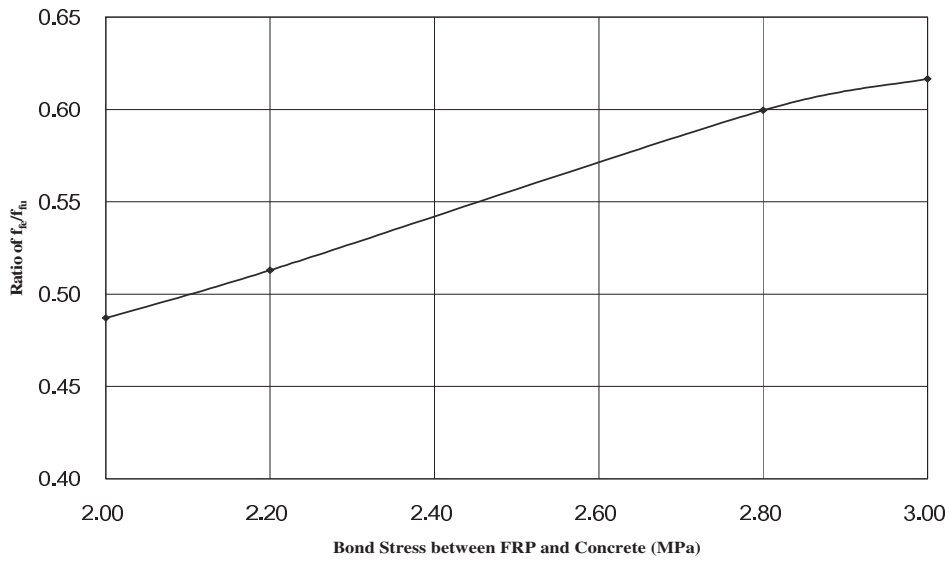


Figure 18 - Relationship of Bond Stress and Value of f_{fc}/f_{fu} (Ductile Bond)

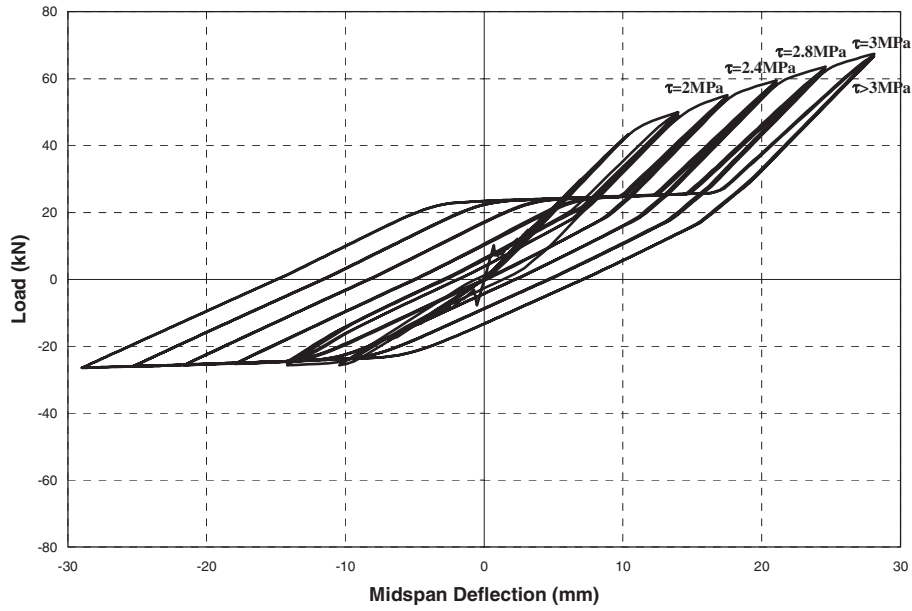


Figure 19 - Cyclic Load- Deformation Response with Different Bond Strength Values

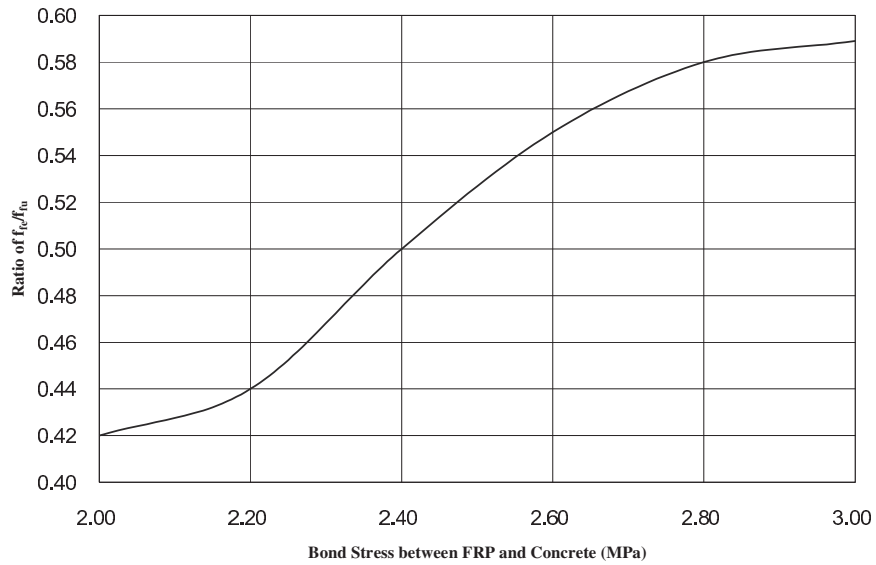


Figure 20 - Relationship of Bond Stress and Value of f_{ie}/f_{iu} (Cyclic Bond)

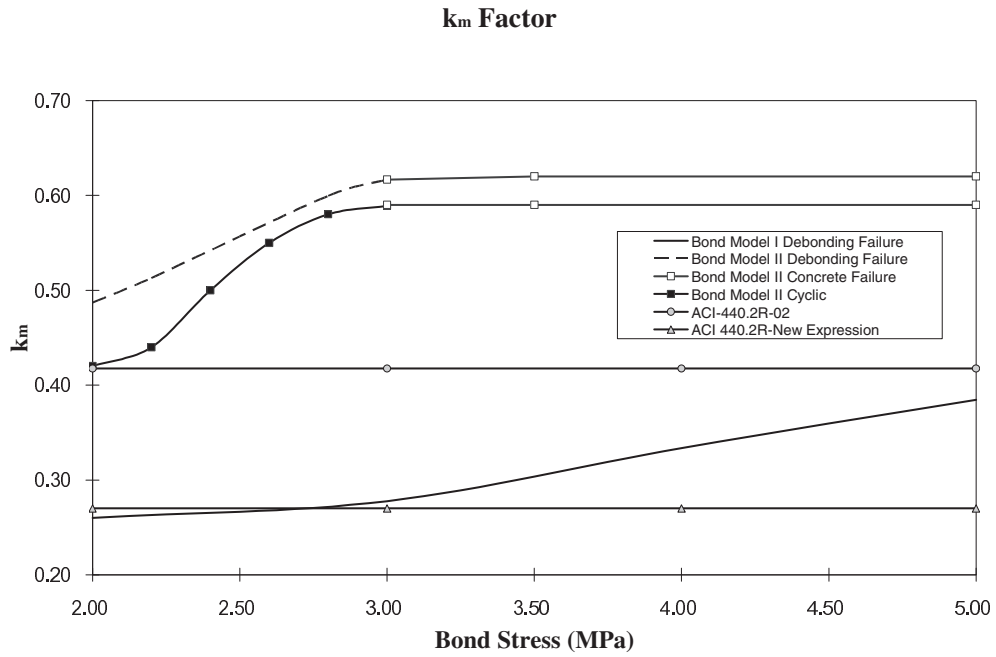


Figure 21 - Influence of Bond Stress on K_m Factor